

Electronic Supporting Information
Continuous Flow Synthesis and Simulation-Supported Investigation of Tunable Plasmonic Gold Patchy Nanoparticles

Julia S. Seifert^{a,b}, Nico Nees^c, Hamzah Khan^d, Nabi E. Traoré^{a,b}, Dominik Drobek^e, Wolfgang Peukert^{a,b}, Benjamin Apeleo Zubiri^e, Erdmann Spiecker^e, Michael Stingl^{c,d}, Lukas Pflug^d, Robin N. Klupp Taylor^{a,b,*}

^a Institute of Particle Technology, Friedrich-Alexander-Universität Erlangen-Nürnberg, Cauerstr. 4, 91058 Erlangen, Germany

^b Interdisciplinary Center for Functional Particle Systems, Friedrich-Alexander-Universität Erlangen-Nürnberg, Haberstr. 9a, 91058 Erlangen, Germany

^c Department of Mathematics, Chair of Applied Mathematics (Continuous Optimization), Friedrich-Alexander-Universität Erlangen-Nürnberg, Cauerstr. 11, 91058 Erlangen, Germany

^d FAU Competence Unit for Scientific Computing (FAU CSC), Friedrich-Alexander-Universität Erlangen-Nürnberg, Martensstr. 5a, 91058 Erlangen, Germany

^e Institute of Micro- and Nanostructure Research (IMN) & Center for Nanoanalysis and Electron Microscopy (CENEM), Friedrich-Alexander-Universität Erlangen-Nürnberg, Interdisciplinary Center for Nanostructured Films (IZNF), Cauerstr. 3, 91058 Erlangen, Germany

*Corresponding author: Robin N. Klupp Taylor: robin.klupp.taylor@fau.de

Double T-Mixer Continuous Flow Set-up

We developed a double T-mixer continuous flow set-up to couple seeding of the core particles and subsequent patch growth in one reaction set-up. A photograph of the set-up is presented in Figure S1.

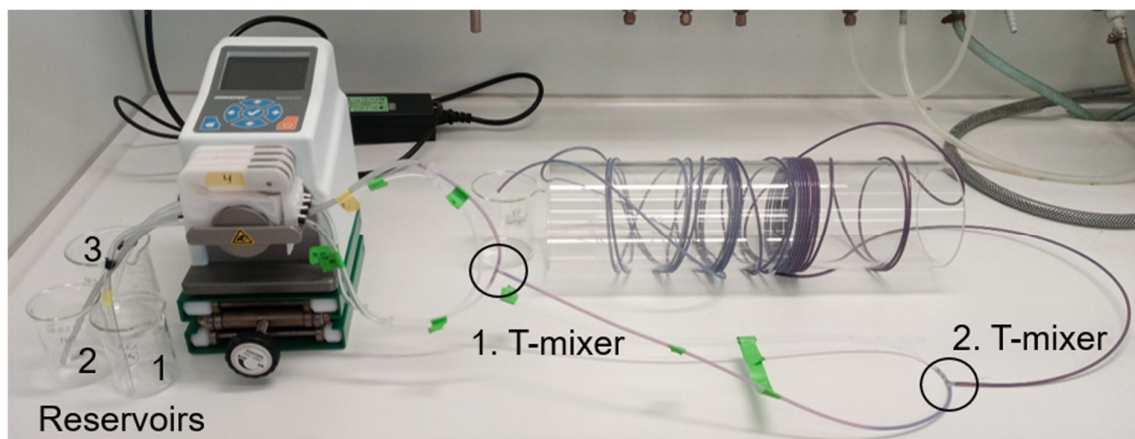


Figure S1: Photograph of the double T-mixer continuous flow set-up.

Densification of Gold Patchy Particles

The influence of the chloride concentration on the patch morphology was investigated in our previously reported non-seeded approach using a single T-mixer continuous flow set-up. Figure S2 shows wide-field SEM micrographs of patchy particle samples synthesized with chloride reagent concentrations ranging from 0 to 120 mM. Here, the change in patch morphology from dendritic to dense patches with increasing chloride concentration can be observed for all particles in the samples.

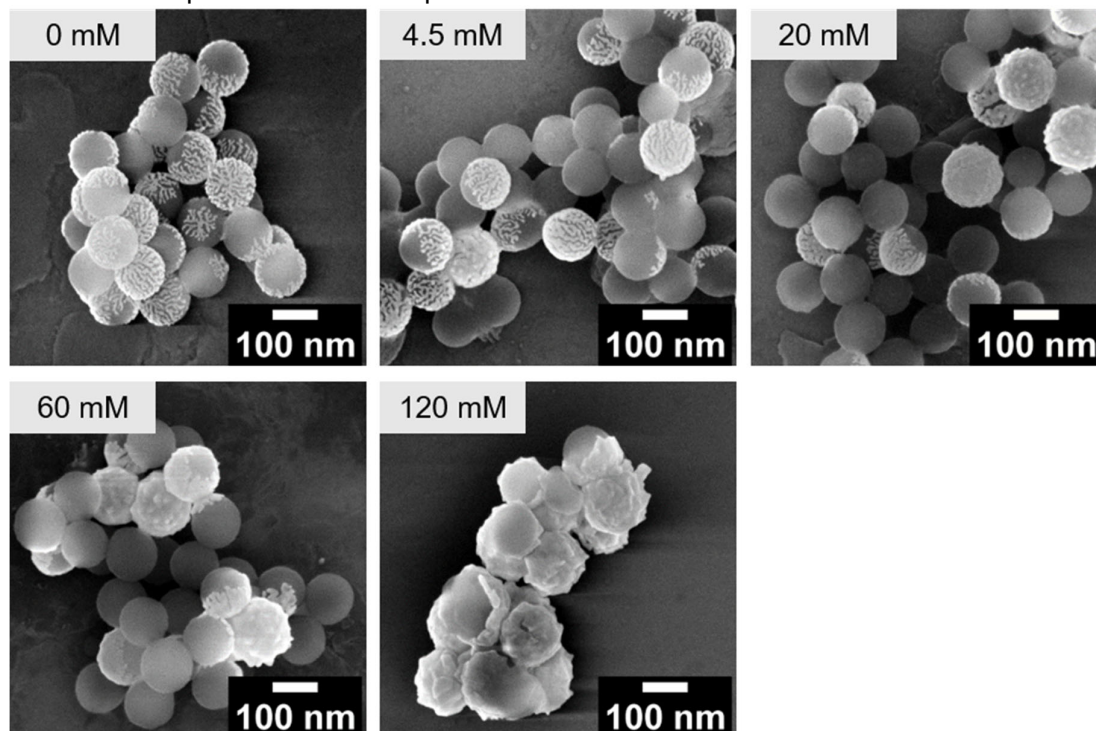


Figure S2: Wide-field SEM micrographs of gold patchy particle samples synthesized using the non-seeded approach (single T-mixer set-up) with varying NaCl content of 0, 4.5, 20, 60 and 120 mM.

Patch Growth on Seeded Core Particles

The introduction of seeds for patch growth is performed by heterocoagulating the cationic core particles with negatively charged gold nanocrystals in continuous flow. For proof-of-principle seeding experiments, the seeding density was set to 1. The successful seeding is visible from the HAADF-STEM micrographs and EDX map in Figure S3. Moreover, the size of the gold nanocrystals can be found to be in the range of 3-6 nm.

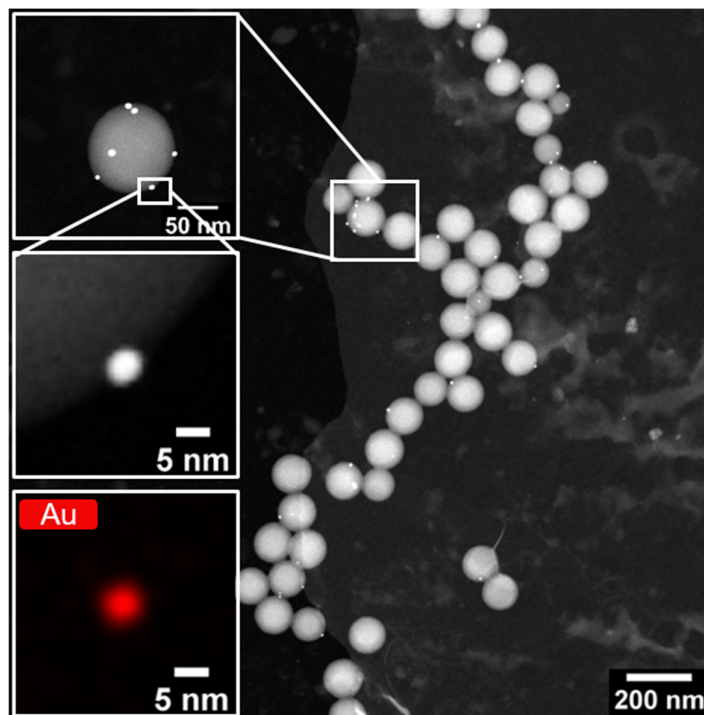


Figure S3: HAADF-STEM micrographs of seeded PS core particles with gold nanocrystals ($\rho_0 = 1$). Insets with enlarged seeded core particles and EDX map of a gold nanocrystal.

Figure S4 shows an extinction spectrum of typical seed nanocrystals (Figure S4a) as well as extinction spectra of bare and seeded core particles (Figure S4b). For the latter spectra, the core concentration corresponds to those in Figure 3 of the main manuscript. In Figure S4b, the scattering of the PS particles clearly dominates the spectrum and due to the very low concentration of gold nanocrystals, their presence is only detectable as a slight shoulder at 500-550 nm for the highest seeding density of 40. Moreover, the extinction levels of the spectra in Figure S4b are many times lower than those of the corresponding samples with grown gold patches in Figure 3. Therefore, we conclude that the optical properties of the gold patches dominate the extinction spectra and if seed nanocrystals that had not grown into a patch were still present, we would not be able to detect them through extinction measurements.

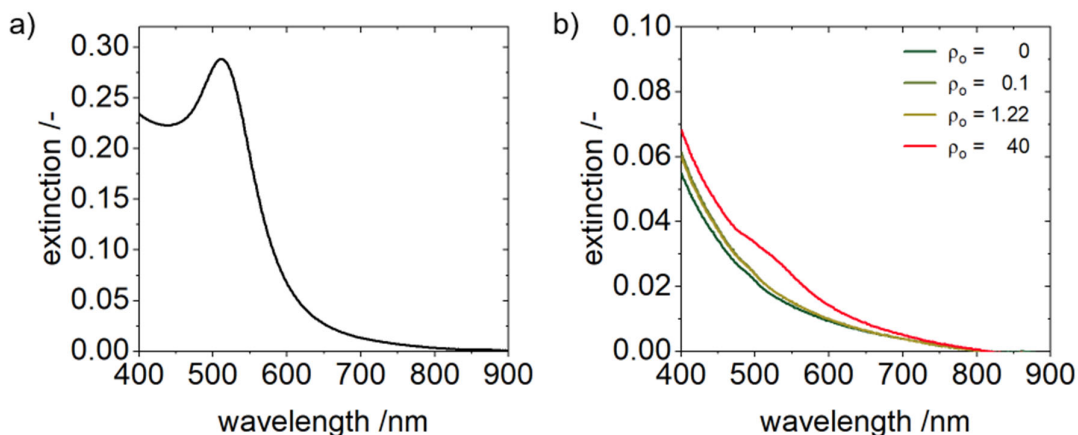


Figure S4: a) Extinction spectrum of gold seed nanocrystals measured four months after synthesis and b) Extinction spectra of seeded core particles (PS115) with seeding densities $\rho_0 = 0, 0.1, 1.22$ and 40 . The core concentration corresponds to that of the patchy particle samples in Figure 3 enabling direct comparison of the extinction levels.

Dense gold patchy particles were synthesized with different seeding densities ($\rho_0 = 0-40$), while the other reagent concentrations were kept constant. Wide-field micrographs in Figure S5 suggest that with an increasing seeding density the number of patches per particle rises and show at the same time that the patch size reduces.

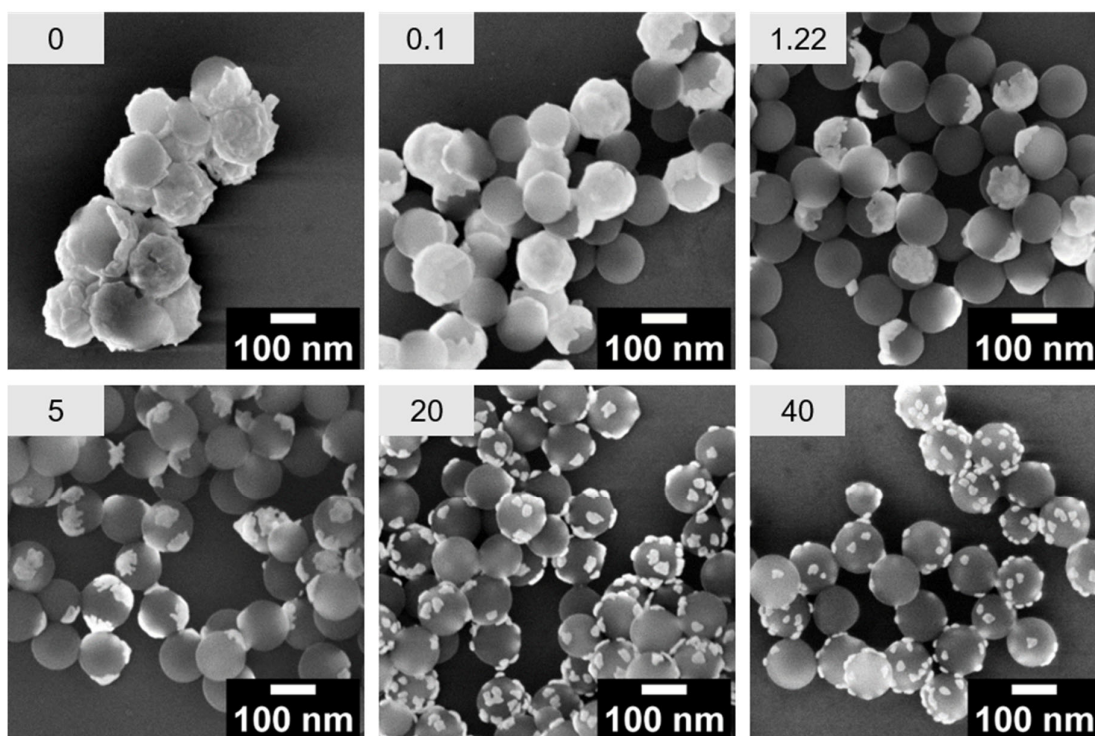


Figure S5: SEM micrographs of gold patchy particle samples synthesized with varying seeding densities $\rho_0 = 0-40$.

Furthermore, Figure S5 reveals that the given seeding density is much higher than the countable number of patches per particle. STEM measurements of a patchy particle sample with seeding density $\rho_0 = 5.81$ reveal some 'free' gold nanoparticles (Figure S6), which are assumed to be seed nanocrystals that have not acted as patch nucleation spots.

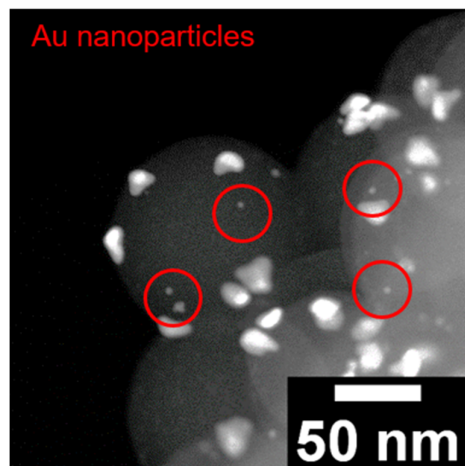


Figure S6: STEM micrograph of a gold patchy particle sample with $\rho_0 = 5.81$. Marked in red are gold nanoparticles, which are assumed to be seed nanocrystals.

Tuning Optical Properties via Reaction Variables

Gold patchy particles synthesis was performed for different values of n^* and constant chloride (120 mM) as well as reducing agent (50 mM) concentration. Figure S7 shows selected extinction spectra of these samples. It shows that with an increasing n^* value the LSPR position shifts to longer wavelengths. Figure S8 presents SEM micrographs of the corresponding samples depicting higher patch coverages for increasing n^* values.

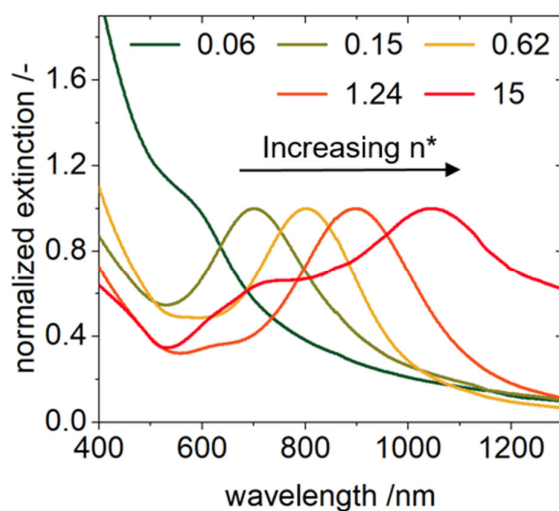


Figure S7: Selected extinction spectra of gold patchy particles synthesized with 120 mM NaCl and 50 mM ascorbic acid concentration and n^* values between 0.06×10^6 and 15×10^6 . Numbers in the legend are multiplied by 10^6 .

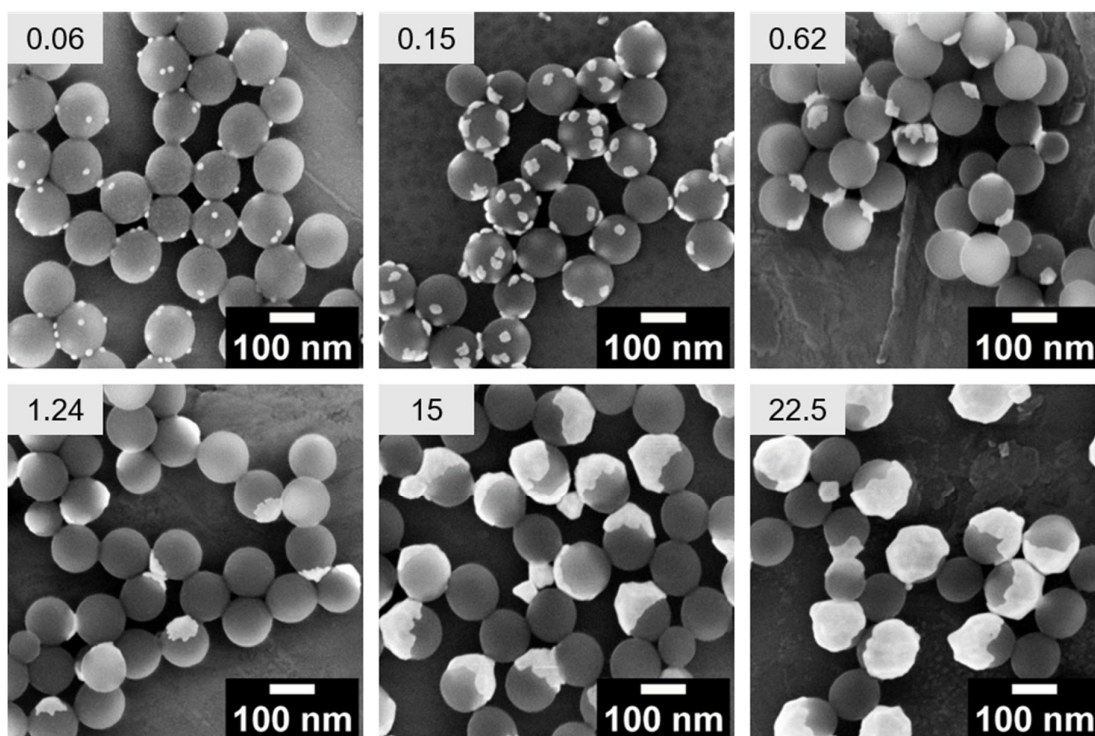


Figure S8: Selected SEM micrographs of gold patchy particles synthesized with 120 mM NaCl and 50 mM ascorbic acid concentration and n^* values between 0.06×10^6 and 22.5×10^6 . Numbers in the micrographs are multiplied by 10^6 .

Moreover, the influence of the chloride and ascorbic acid concentration on the n^* -peak position relationship was tested. For higher NaCl (300 mM) and lower ascorbic acid concentrations (4 mM) a shift of the resonance position to shorter wavelengths was observed (Figure 4c and d). SEM micrographs in Figure S9 reveal that, for both cases, the patches become smaller and appear to be thicker explaining the blue shift of their dipolar resonance positions.

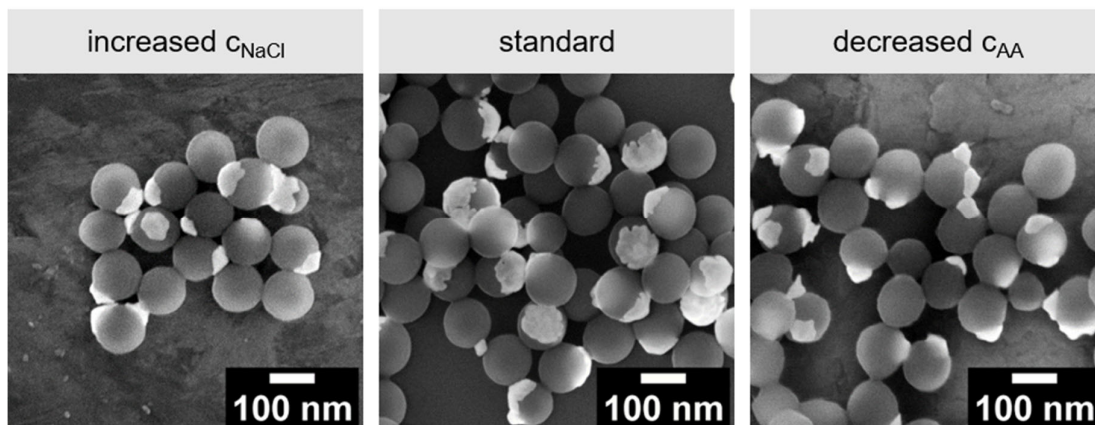


Figure S9: SEM micrographs of gold patchy particles with $n^* = 2.47 \times 10^6$ and different chloride and ascorbic acid concentrations. The standard concentrations (middle micrograph) were set to be 120 mM NaCl and 50 mM ascorbic acid in the reactant. The left micrograph shows a sample with 300 mM NaCl and 50 mM ascorbic acid concentration, the right micrograph a sample with 120 mM NaCl and 4 mM ascorbic acid concentration.

Investigation of Gold Patch Morphology via FEM Simulations

During model development for the electrodynamic simulations of the gold patchy particles, different shape models were explored. Figure S10 shows the schematics of the parametrization of the elliptical and the curved cone patch models. Parameters marked in red are initially defined and partly experimentally derived input parameters for the FEM simulations. The blue parameters can be calculated by the mathematical descriptions given below (Equation (S1)-(S11)). In both cases, the PS core particle size is described by the radius r_c , the patch coverage (cov) by an angle θ and the patch edge radius by r_s . For the elliptical model, the patch height h is defined by an angle α (Figure S10a). The latter describes under which angle the circle with radius r_s tangentially touches the ellipse with the semi-axis a and b . For $\alpha = 0$, the patch will have a constant thickness, for values $\alpha > 0$ (here: 0.5) the patch will be elliptical. In the curved cone model, the length r_t describes the distance from the theoretical tip of the cone to the point where the tip curvature circle, defined by r_w , touches tangentially the patch sideline.

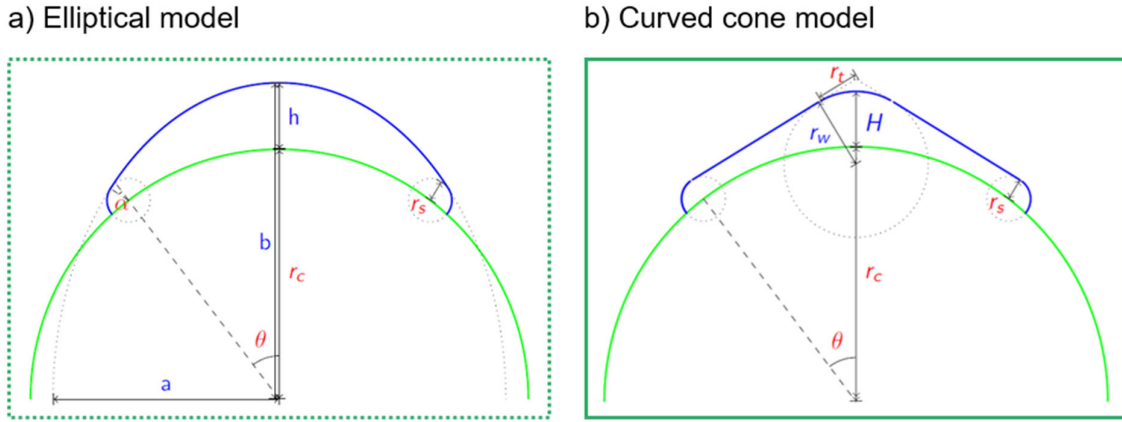


Figure S10: Schematics of the parametrization of the patch shape models for the FEM simulations: a) elliptical and b) curved cone model.

General mathematical description

The angle θ given by Equation (S1) defines the patch coverage. It determines the position of the edge radius circle with radius r_s on the core particles' surface:

$$\theta = \begin{cases} \arccos(-1), & \text{if } cov == 1 \\ \arccos(1 - 2cov) - \arccos(1 - \frac{r_s^2}{2r_c^2}), & \text{else} \end{cases} \quad (S1)$$

Elliptical model description

First, the semi-axis of the ellipse a and b are calculated by Equation (S2) and (S3):

$$a^2 = x^2 + y^2 \cdot \frac{y - y_0}{x - x_0} \cdot \frac{x}{y} \quad (S2)$$

$$b^2 = \frac{x - x_0}{y - y_0} \cdot \frac{y}{x} \cdot a^2 \quad (S3)$$

Whereby the variables x_0 , y_0 , x and y are defined as shown in Equations (S4)-(S7):

$$x_0 = r_c \cdot \cos\left(\frac{\pi}{2} + \theta\right) \quad (\text{S4})$$

$$y_0 = r_c \cdot \sin\left(\frac{\pi}{2} + \theta\right) \quad (\text{S5})$$

$$x = x_0 + r_s \cdot \cos\left(\frac{\pi}{2} + \theta + \alpha\right) \quad (\text{S6})$$

$$y = y_0 + r_s \cdot \sin\left(\frac{\pi}{2} + \theta + \alpha\right) \quad (\text{S7})$$

Due to a 90° rotation of the ellipse, the result for a^2 has to be inserted for the b semiaxis and vice versa.

The elliptical patch height h is calculated by Equation (S8):

$$h = b - r_c \quad (\text{S8})$$

Curved cone model description

For the curved cone model, the tip radius r_w is given by Equation (S9):

$$r_t = \sqrt{\left(\frac{r_w}{\sin(\gamma)}\right)^2 - r_w^2} \quad (\text{S9})$$

The angle γ describes the opening angle of the theoretical cone with Equation (S10):

$$\gamma = \arctan\left(\frac{x_0}{r_c + h - y_0}\right) + \arcsin\left(\frac{r_s}{\sqrt{x_0^2 + (r_c - h - y_0)^2}}\right) \quad (\text{S10})$$

Here, h is the height from the core particle's surface to the theoretical tip of the cone. x_0 and y_0 are defined by Equations (S4) and (S5).

The height of the curved cone patch H can finally be calculated by Equation (S11):

$$H = h - \left(\frac{r_w}{\sin(\gamma)} - r_w\right) \quad (\text{S11})$$

Then, we explored the structure-property relationship for gold patchy particles by investigating the influence of the different shape parameters on the optical properties. In Figure S11, the complementary results to Figure 6 are presented. Here, the influence of the tip curvature radius shows to have no influence on the optical spectra.

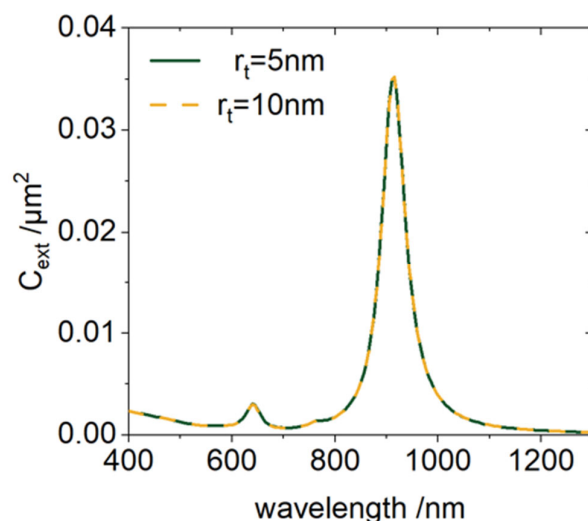


Figure S11: Simulated extinction spectra of patches with the curved cone model for varied tip curvature radius of 5 and 10 nm and 13% coverage, $H = 15.3$ nm, $r_s = 5$ nm.

For the curved cone model, the experimentally observed spectral data show good agreement with the corresponding simulated spectra for patches with different coverages and thicknesses (Figure S12). The dimensions of the experimental samples obtained by image analysis and the chosen simulated parameters are listed in Table S1.

Table S1: Dimensions of the experimental and simulated samples.

| Experiment | | Simulation | | |
|-------------|-----------------------|-------------|---------------------------|-----------------------|
| Coverage /% | Central thickness /nm | Coverage /% | Central thickness H /nm | Edge radius r_s /nm |
| 3 ± 2 | 11 ± 6 | 2 | 10 | 2 |
| 5 ± 2 | 10 ± 5 | 4 | 10 | 2 |
| 6 ± 2 | 10 ± 7 | 6 | 10 | 2 |
| 13 ± 4 | 18 ± 8 | 13 | 20 | 2 |

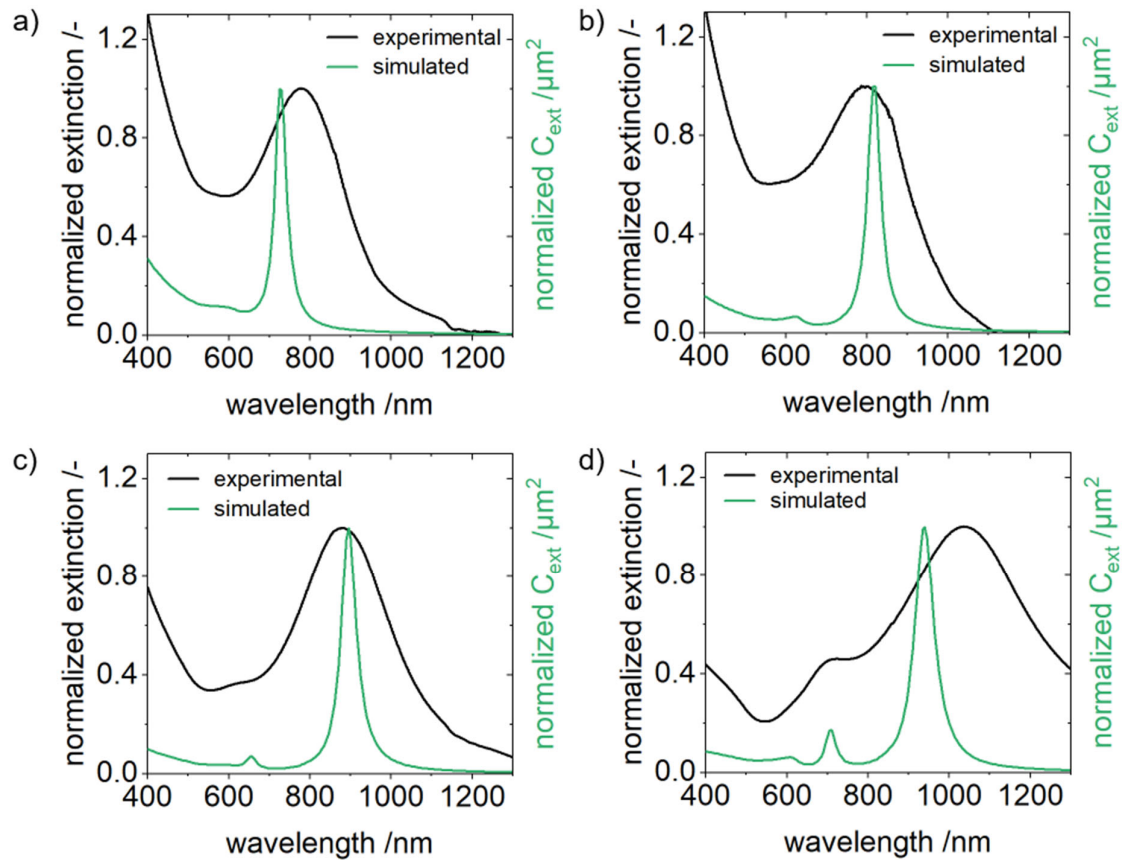


Figure S12: Comparison of experimental extinction spectra of a patchy particle sample with a) $3 \pm 2\%$, b) $5 \pm 2\%$, c) $6 \pm 2\%$ and d) $13 \pm 4\%$ coverage (black) and simulated extinction spectra of a patch with corresponding coverage and central thickness with the curved cone model (green). The exact parameters are given in Table S1.

Elucidation of the Effect of Post-Synthesis Ageing on Patch Shape and Optical Properties

In order to understand the time-dependent change in the optical properties of the patchy particles after synthesis, supporting SEM micrographs were taken on the day of synthesis and one week after (Figure S13). Sucrose addition was always performed directly after the synthesis. This retains the patch structure in a curved cone shape, which is revealed at day 1 and one week after synthesis (see Figure S13 left and middle). In contrast, the as-prepared sample exhibits more spherical, elliptical patches one week after synthesis (see Figure S13 right).

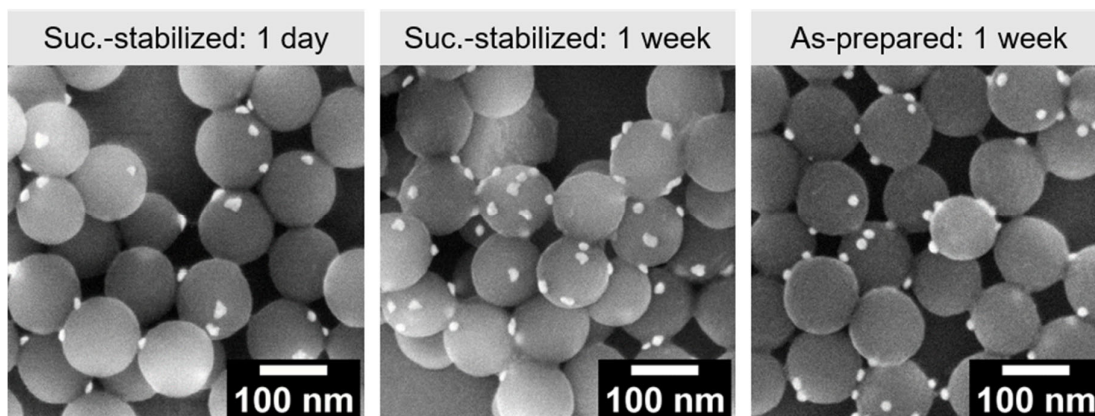


Figure S13: SEM micrographs of differently treated gold patchy particles. Left: particles with sucrose at day 1 after synthesis; middle: particles with sucrose one week after synthesis; right: as-prepared particles one week after synthesis.